Supplementary information

Structure, electrical conductivity and oxygen transport properties of Ruddlesden-Popper phases $Ln_{n+1}Ni_nO_{3n+1}$ (*Ln* = La, Pr and Nd; *n* = 1, 2 and 3)

Jia Song,[a] De Ning,[b] Bernard Boukamp,[c] Jean-Marc Bassat,[d] and Henny J.M. Bouwmeester*[a, e, f]

[a]*Electrochemistry Research Group, Membrane Science and Technology, MESA+ Institute for Nanotechnology, University of Twente, P.O. Box 217, 7500 AE, Enschede, The Netherlands*

[b]*Helmholtz-Zentrum Berlin für Materialien und Energie, Hahn-Meitner-Platz 1, 14109 Berlin, Germany*

[c]*Inorganic Materials Science, MESA+ Institute for Nanotechnology, University of Twente, P.O. Box 217, 7500 AE, Enschede, The Netherlands*

[d]*CNRS, Université de Bordeaux, Institut de Chimie de la Matière Condensée de Bordeaux (ICMCB), 87 Av. Dr Schweitzer, F-33608 Pessac Cedex, France*

[e]*CAS Key Laboratory of Materials for Energy Conversion, Department of Materials Science and Engineering, University of Science and Technology of China, Hefei, 230026, P. R. China*

[f]*Forschungszentrum Jülich GmbH, Institute of Energy and Climate Research-IEK-1, Leo- Brandt-Str. 1, D-52425, Jülich, Germany*

Table S1 — Structural parameters for different RP nickelates as determined by Rietveld refinements of powder XRD data collected at room temperature.

Atom	Site	x	y	z	B	occ
$La_2NiO_{4+\delta}$	***Fmmm*, *a* = 5.4612(5) Å, *b* = 5.4607(5) Å, *c* = 12.6772(1) Å**					
La	8i	0	0	0.3609(1)	2.38(4)	1
Ni	4a	0	0	0	2.7(1)	1
O1	8e	0.25	0.25	0	1.9(2)	1
O2	8i	0	0	0.1729(8)	4.5(2)	1
O3	8f	0.25	0.25	0.25	0.1(1)	0.040
$Nd_2NiO_{4+\delta}$	***Fmmm*, *a* = 5.44647(7) Å, *b* = 5.37712(7) Å, *c* = 12.36234(18) Å**					
Nd	8i	0	0	0.3592(1)	1.97(4)	1
Ni	4a	0	0	0	1.9(1)	1
O1	8e	0.25	0.25	0	1.8(3)	1
O2	8i	0	0	0.1726(10)	6.6(3)	1
O3	8f	0.25	0.25	0.25	0.1(1)	0.052
$La_3Ni_2O_{7-\delta}$	***Cmmm*, *a* = 5.39491(5) Å, *b* = 5.45054(5) Å, *c* = 20.53039(25) Å**					
La1	2a	0	0	0	0.1(1)	1
La2	2c	0	0.5	0.5	0.44(9)	1
La3	4l	0	0.5	0.3189(2)	0.1(1)	1
La4	4k	0	0	0.1806(3)	0.8(1)	1
Ni1	4k	0	0	0.3976(5)	0.9(4)	1
Ni2	4l	0	0.5	0.0930(5)	0.2(3)	1
O1	2b	0	0.5	0	21(1)	1
O2	2d	0	0	0.5	0.1(1)	1
O3	4k	0	0	0.2861(12)	0.1(1)	1
O4	4l	0	0.5	0.1704(14)	4.7(9)	1
O5	8m	0.25	0.25	0.4097(15)	3(1)	1
O6	8m	0.25	0.25	0.1022(13)	0.7(8)	1

Table S1 *contd*. — Structural parameters for different RP nickelates as determined by Rietveld refinements of powder XRD data collected at room temperature.

Atom	Site	x	y	z	B	occ
$La_4Ni_3O_{10-\delta}$	***P2₁a*, *a* = 5.41585(6) Å, *b* = 5.46551(6) Å, *c* = 27.97613(41) Å, β = 90.184(1)**					
La1	4e	-0.0061(17)	0.0087(19)	0.3015(1)	0.1(1)	1
La2	4e	0.4803(23)	-0.0109(26)	0.8011(2)	3.5(1)	1
La3	4e	-0.0099(22)	-0.0036(24)	0.4339(2)	1.2(1)	1
La4	4e	0.4929(22)	-0.0228(23)	0.9289(2)	2.4(2)	1
Ni1	2a	0	0	0	5.1(8)	1
Ni2	2b	0	0.5	0.5	3.8(7)	1
Ni3	4e	0.0036(48)	-0.0120(45)	0.1341(4)	1.7(2)	1
Ni4	4e	0.4840(35)	0.0084(44)	0.6444(3)	0.1(1)	1
O1	4e	0.301(16)	0.283(16)	0.493(3)	0.1(1)	1
O2	4e	0.294(13)	0.198(14)	0.992(2)	0.1(1)	1
O3	4e	-0.010(14)	0.019(14)	0.067(1)	0.1(1)	1
O4	4e	0.510(10)	0.012(14)	0.597(1)	0.1(1)	1
O5	4e	0.246(15)	0.254(18)	0.136(2)	0.1(1)	1
O6	4e	0.960(8)	0.014(15)	0.610(1)	0.1(1)	1
O7	4e	0.020(11)	0.022(16)	0.214(1)	0.1(1)	1
O8	4e	0.468(10)	-0.008(20)	0.697(1)	0.1(1)	1
O9	4e	0.793(11)	0.184(11)	0.894(1)	0.1(1)	1
O10	4e	0.223(12)	0.206(12)	0.375(1)	0.1(1)	1

Table S1 *contd*. — Structural parameters for different RP nickelates as determined by Rietveld refinements of powder XRD data collected at room temperature.

Atom	Site	x	y	z	B	occ
$Pr_4Ni_3O_{10-\delta}$	***P2₁a*, *a* = 5.37714(7) Å, *b* = 5.46620(9) Å, *c* = 27.55933(51) Å, β = 90.236(1)**					
Pr1	4e	-0.0025(20)	0.0006(42)	0.2998(4)	0.5(1)	1
Pr2	4e	0.4999(20)	0.0020(43)	0.8010(4)	0.1(1)	1
Pr3	4e	-0.0252(15)	0.0064(46)	0.4321(4)	0.1(1)	1
Pr4	4e	0.5012(16)	0.0060(47)	0.9306(4)	0.2(1)	1
Ni1	2a	0	0	0	0.1(1)	1
Ni2	2b	0	0.5	0.5	0.1(1)	1
Ni3	4e	0.000(5)	0.011(10)	0.1347(6)	0.1(1)	1
Ni4	4e	0.4972(47)	0.0002(93)	0.6437(5)	0.1(1)	1
O1	4e	0.234(22)	0.240(22)	0.516(2)	0.1(1)	1
O2	4e	0.194(16)	0.285(16)	1.001(4)	0.1(1)	1
O3	4e	-0.003(16)	-0.053(20)	0.067(3)	0.1(1)	1
O4	4e	0.506(15)	-0.102(26)	0.575(2)	0.1(1)	1
O5	4e	0.227(25)	0.288(37)	0.131(3)	0.1(1)	1
O6	4e	0.736(20)	0.223(18)	0.608(3)	0.1(1)	1
O7	4e	0.000(19)	0.092(22)	0.214(3)	0.1(1)	1
O8	4e	0.497(18)	0.070(22)	0.720(3)	0.1(1)	1
O9	4e	0.753(33)	0.193(44)	0.859(5)	0.1(1)	1
O10	4e	0.223(12)	0.206(12)	0.357(4)	0.1(1)	1

Table S1 *contd*. — Structural parameters for different RP nickelates as determined by Rietveld refinements of powder XRD data collected at room temperature.

Atom	Site	x	y	z	B	occ
$Nd_4Ni_3O_{10-\delta}$	***$P2_1a$*, *a* = 5.36486(4) Å, *b* = 5.45342(6) Å, *c* = 27.41622(32) Å, β = 90.296(1)**					
Nd1	4e	0.0016(16)	0.0109(22)	0.2989(2)	0.7(1)	1
Nd2	4e	0.5019(14)	0.0135(22)	0.8011(2)	0.1(1)	1
Nd3	4e	-0.0346(10)	0.0034(19)	0.4332(2)	0.1(1)	1
Nd4	4e	0.4893(11)	0.0024(20)	0.9293(2)	0.3(2)	1
Ni1	2a	0	0	0	0.1(8)	1
Ni2	2b	0	0.5	0.5	2.2(7)	1
Ni3	4e	0.0111(33)	0.0114(50)	0.1375(5)	0.1(2)	1
Ni4	4e	0.4974(30)	0.0107(47)	0.6436(4)	0.3(1)	1
O1	4e	0.235(16)	0.293(18)	0.510(2)	0.1(1)	1
O2	4e	0.255(22)	0.234(26)	1.009(2)	0.1(1)	1
O3	4e	-0.047(6)	-0.091(9)	0.060(1)	0.1(1)	1
O4	4e	0.522(7)	-0.063(10)	0.576(1)	0.1(1)	1
O5	4e	0.220(13)	0.248(16)	0.141(1)	0.1(1)	1
O6	4e	0.728(10)	0.235(9)	0.616(1)	0.1(1)	1
O7	4e	0.000(10)	-0.030(9)	0.211(1)	0.1(1)	1
O8	4e	0.506(10)	0.097(8)	0.722(1)	0.1(1)	1
O9	4e	0.741(16)	0.268(16)	0.858(1)	0.1(1)	1
O10	4e	0.239(10)	0.282(11)	0.340(1)	0.1(1)	1

Table S2 — Lattice parameters and reliability factors obtained from the Rietveld refinements of room temperature XRD patterns of the ECR samples.

	$La_3Ni_2O_{7-\delta}$	$La_4Ni_3O_{10-\delta}$	$Pr_4Ni_3O_{10-\delta}$	$Nd_4Ni_3O_{10-\delta}$
Space group	*Cmmm*	$P2_1a$	$P2_1a$	$P2_1a$
***a*/ Å**	5.4048(2)	5.4144(1)	5.3721(1)	5.3648(1)
***b*/ Å**	5.4489(2)	5.4586(1)	5.4535(1)	5.4440(1)
***c*/ Å**	20.493(1)	27.9955(8)	27.576(1)	27.486(1)
β/ °	90	90.247(3)	90.276(3)	90.335(3)
***V*/ Å^3**	603.540(2)	827.410(1)	809.935(1)	802.774(1)
R_{wp}/ %	20.5	15.4	16.3	17.7
R_{exp}/ %	3.93	3.62	4.64	5.01
R_{Bragg}/%	8.01	7.82	10.3	11.0
χ^2/ -	27.2	15.3	12.3	12.5

Table S3 — Comparison of the electrical conductivity (at 750 °C in air) and sample density of $La_3Ni_2O_{7-\delta}$, $La_4Ni_3O_{10-\delta}$, $Pr_4Ni_3O_{10-\delta}$, and $Nd_4Ni_3O_{10-\delta}$ from this work with corresponding data reported in literature.

	This work		**Literature**		
	σ_{ion} (S cm^{-1})	**Relative density (%)**	σ_{ion} (S cm^{-1})	**Relative density (%)**	**Ref.**
$La_3Ni_2O_{7-\delta}$	241.99	96.8	58.0	58	[33]
			60.0	Porous	[66]
			51.6	Porous	[35]
			90.0	Porous	[13]
$La_4Ni_3O_{10-\delta}$	419.15	96.1	89.0	58	[33]
			93.1	56	[67]
			89.7	Porous	[35]
			174.9	Porous	[13]
$Pr_4Ni_3O_{10-\delta}$	322.74	96.4	85.0	70	[4]
$Nd_4Ni_3O_{10-\delta}$	375.54	97.3	N.A.	N.A.	

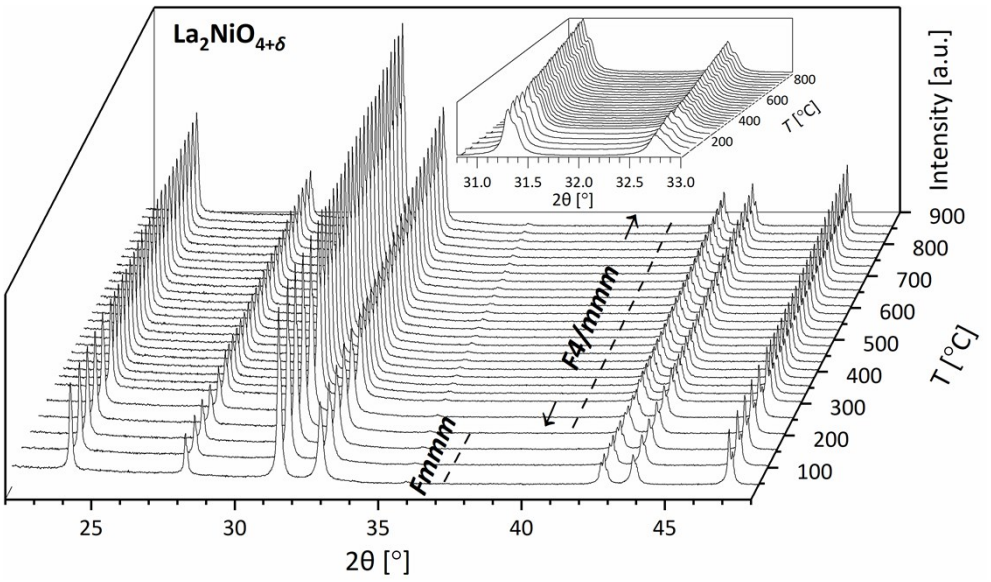

Figure S1 — *In situ* HT-XRD patterns for $La_2NiO_{4+\delta}$ (powder) between 22° and 48° recorded in air from 40°C to 1000 °C, showing a phase transition from orthorhombic *Fmmm* to tetragonal *F4/mmm* at approx. 175 °C. The inset shows a magnification of the peaks between 30.8° – 33.0°.

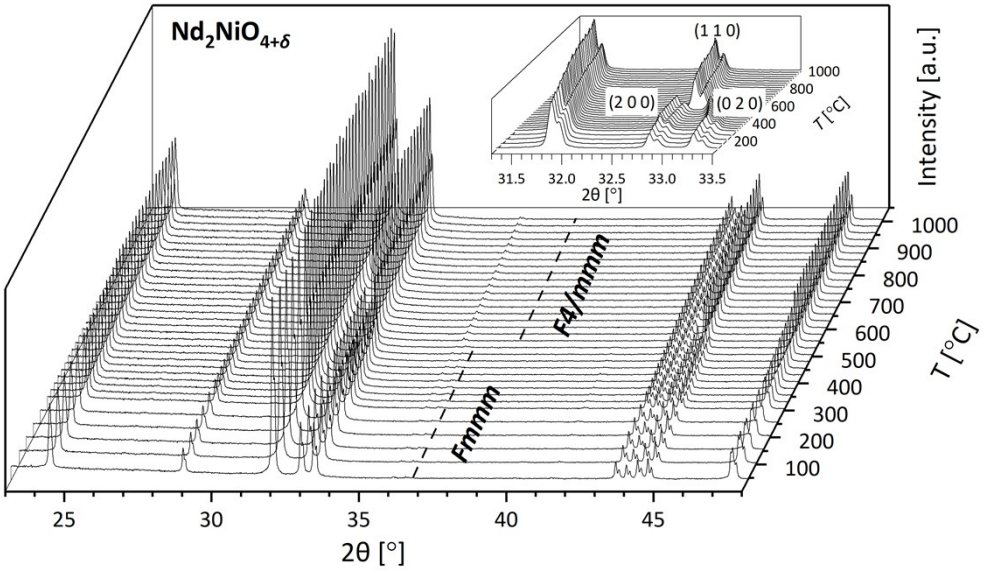

Figure S2 — *In situ* HT-XRD patterns for $Nd_2NiO_{4+\delta}$ (powder) between 22° and 48° recorded in air from 40°C to 1000 °C, showing a phase transition from orthorhombic *Fmmm* to tetragonal *F4/mmm* at approx. 750 °C. The inset shows a magnification of the peaks between 30.8° – 33.5°. Note the merging of (0 2 0) and (2 0 0) peaks in the *Fmmm* phase to the (1 1 0) peak in the *F4/mmm* phase.

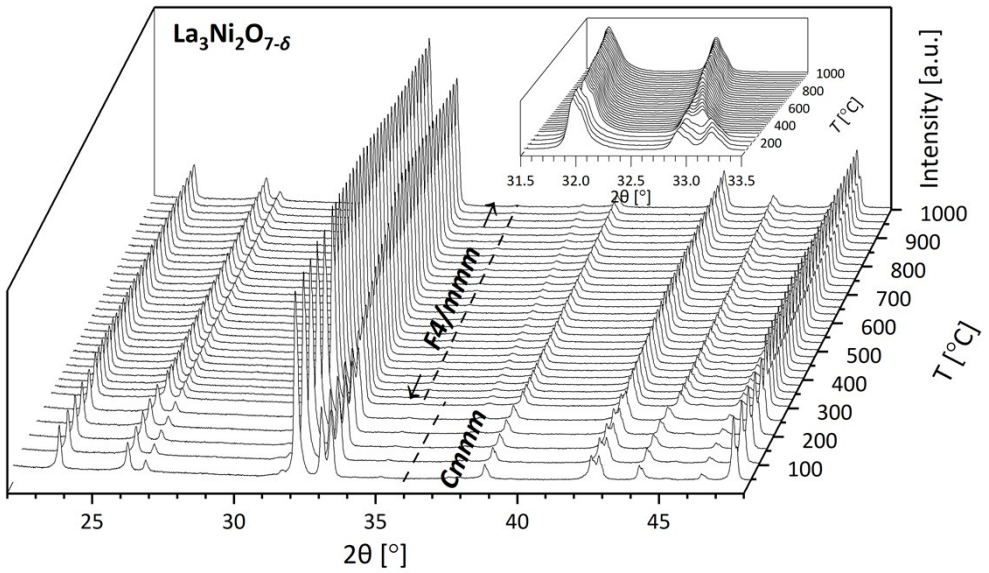

Figure S3 — *In situ* HT-XRD patterns for $La_3Ni_2O_{7-\delta}$ (powder) between 22° and 48° recorded in air from 40°C to 1000 °C, showing the transition from orthorhombic *Cmmm* to tetragonal *F4/mmm* at approx. 300 °C. The inset shows a magnification of the peaks between 31.5° – 33.5°.

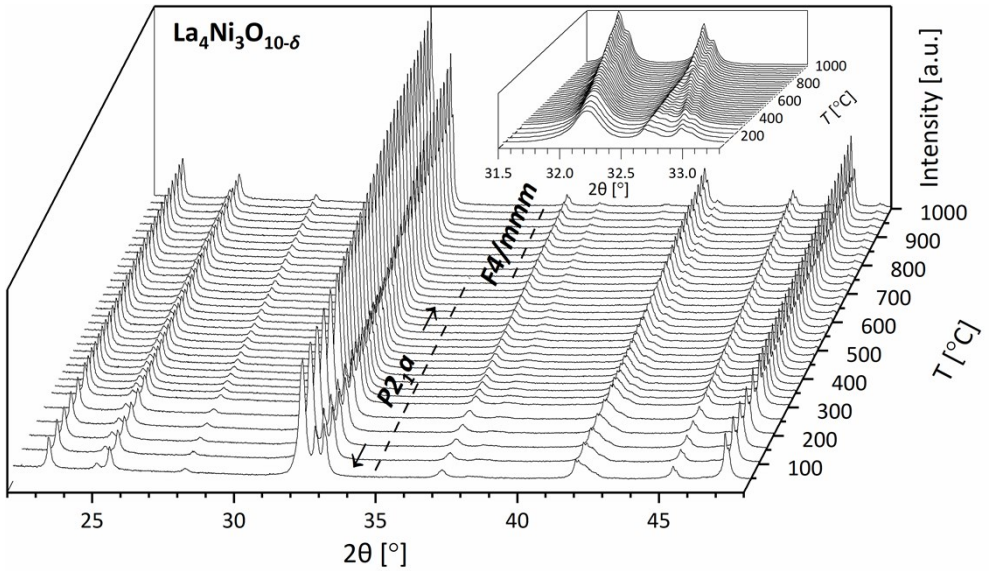

Figure S4 — *In situ* HT-XRD patterns for $La_4Ni_3O_{10-\delta}$ (powder) between 22° and 48° recorded in air from 40°C to 1000 °C, showing the transition from monoclinic $P2_1a$ to tetragonal *F4/mmm* at approx. 750 °C. The inset shows a magnification of the peaks between 31.5° – 33.3°.

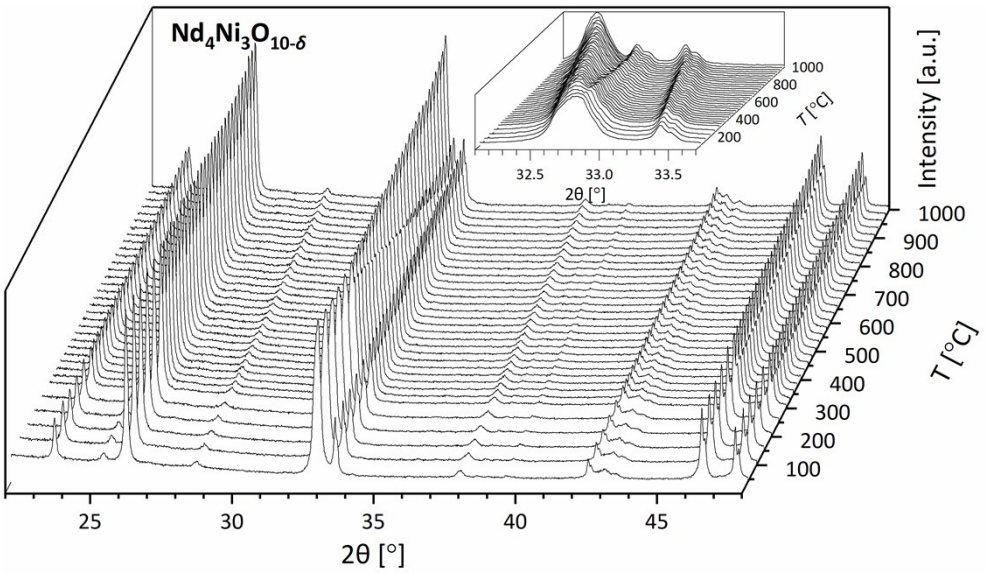

Figure S5 — *In situ* HT-XRD patterns for $Nd_4Ni_3O_{10-\delta}$ (powder) between 22° and 48° recorded in air from 40°C to 1000 °C. The structure remains monoclinic $P2_1a$ up to 1000 °C. The inset shows a magnification of the peaks between 32.1° – 33.7°.

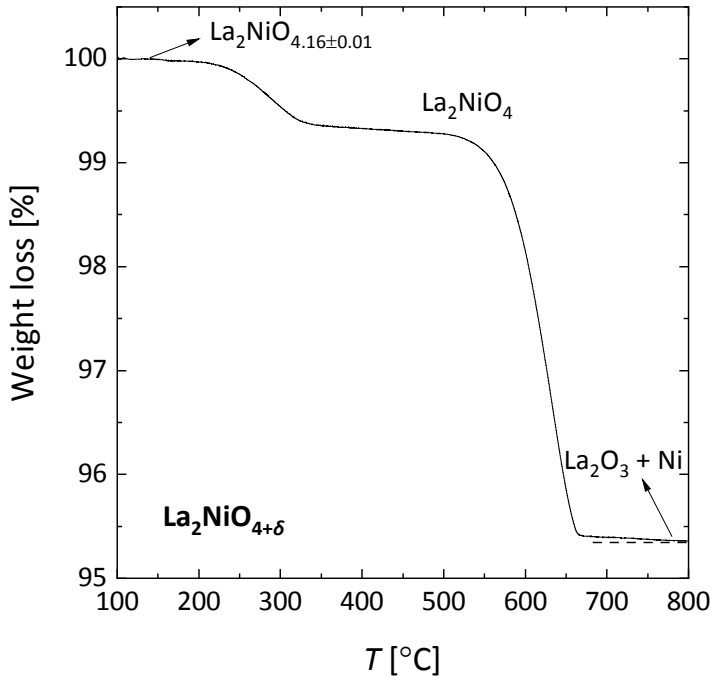

Figure S6 —Weight loss curve for $La_2NiO_{4+\delta}$ in 16% H_2/Ar.

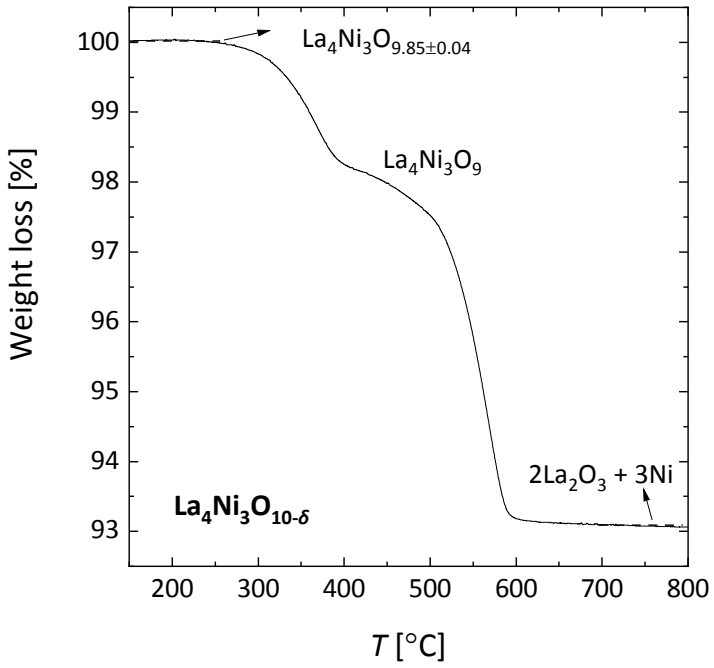

Figure S7 — Weight loss curve for $La_4Ni_3O_{10-\delta}$ in 16% H_2/Ar.

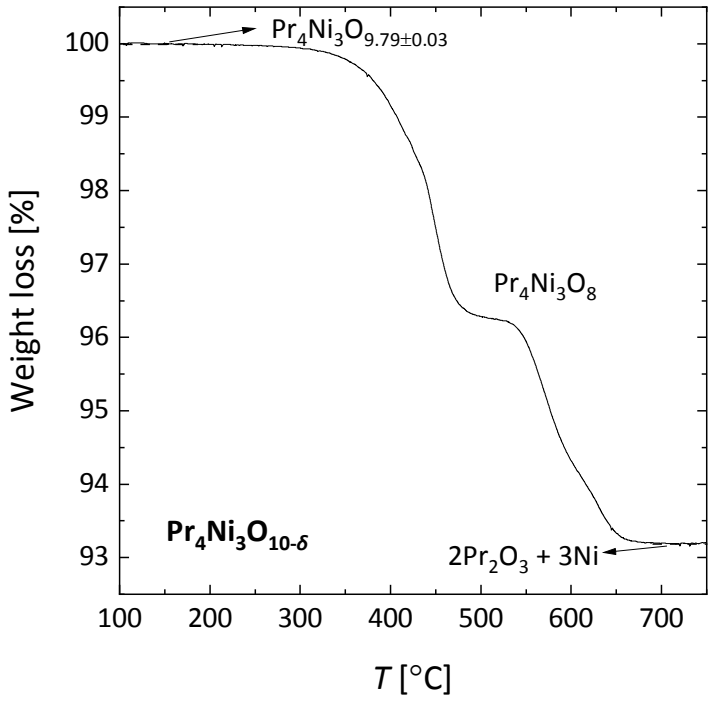

Figure S8 — Weight loss curve for $Pr_4Ni_3O_{10-\delta}$ in 16% H_2/Ar.

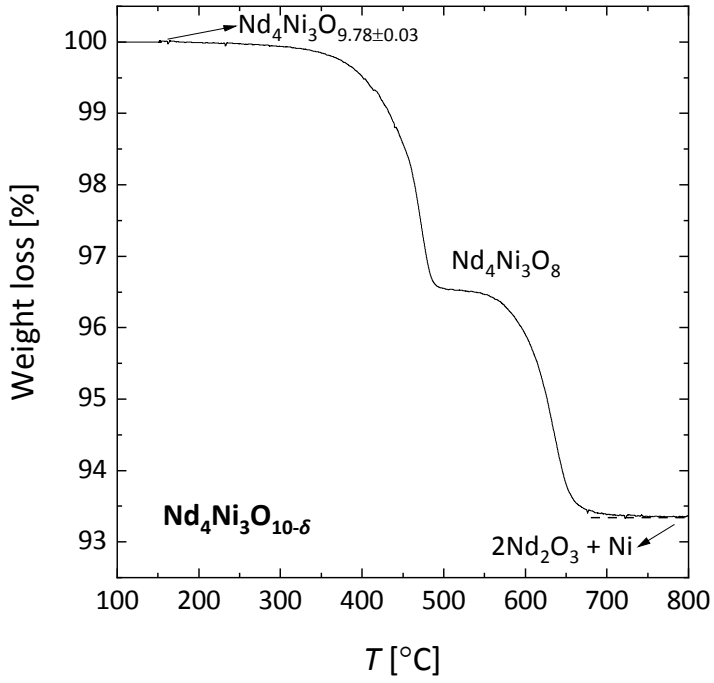

Figure S9 — Weight loss curve for $Nd_4Ni_3O_{10-\delta}$ in 16% H_2/Ar.

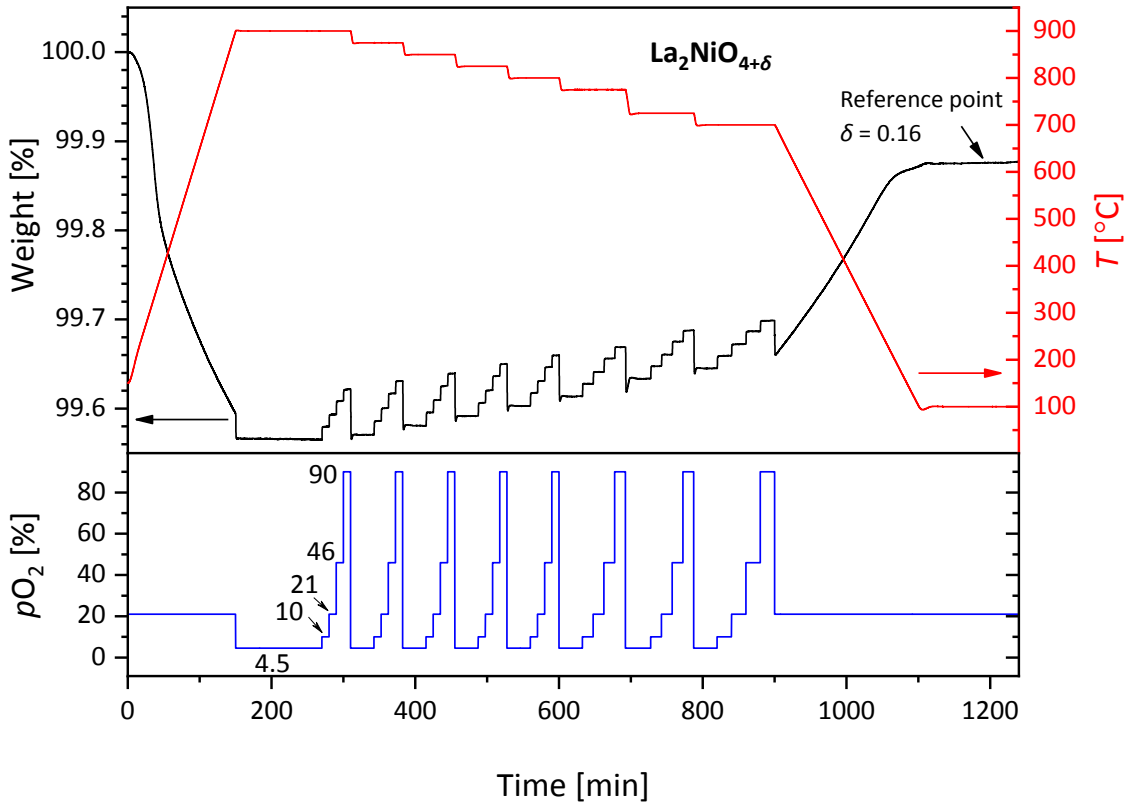

Figure S10 — Weight loss curve for $La_2NiO_{4+\delta}$ on cooling from 900 °C to 700 °C, with intervals of 25 °C, at different pO_2 values. The reference point was selected after equilibration for 3 h at T = 100 °C and pO_2 = 0.21 bar. The corresponding value (δ = 0.16) was determined by reduction in hydrogen (16% H_2/Ar).

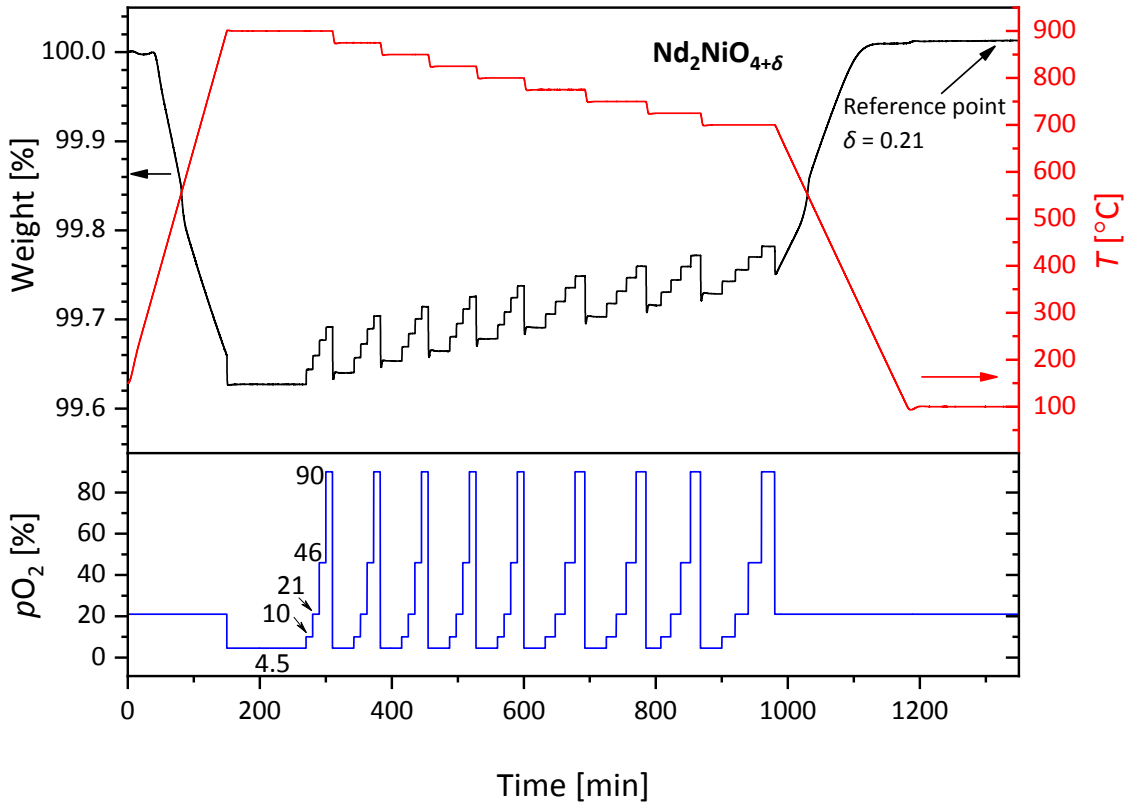

Figure S11 — Weight loss curve for $Nd_2NiO_{4+\delta}$ on cooling from 900 °C to 700 °C, with intervals of 25 °C, at different pO_2 values. The reference point was selected after equilibration for 3 h at T = 100 °C and pO_2 = 0.21 bar. The corresponding value (δ = 0.21) was determined by reduction in hydrogen (16% H_2/Ar).

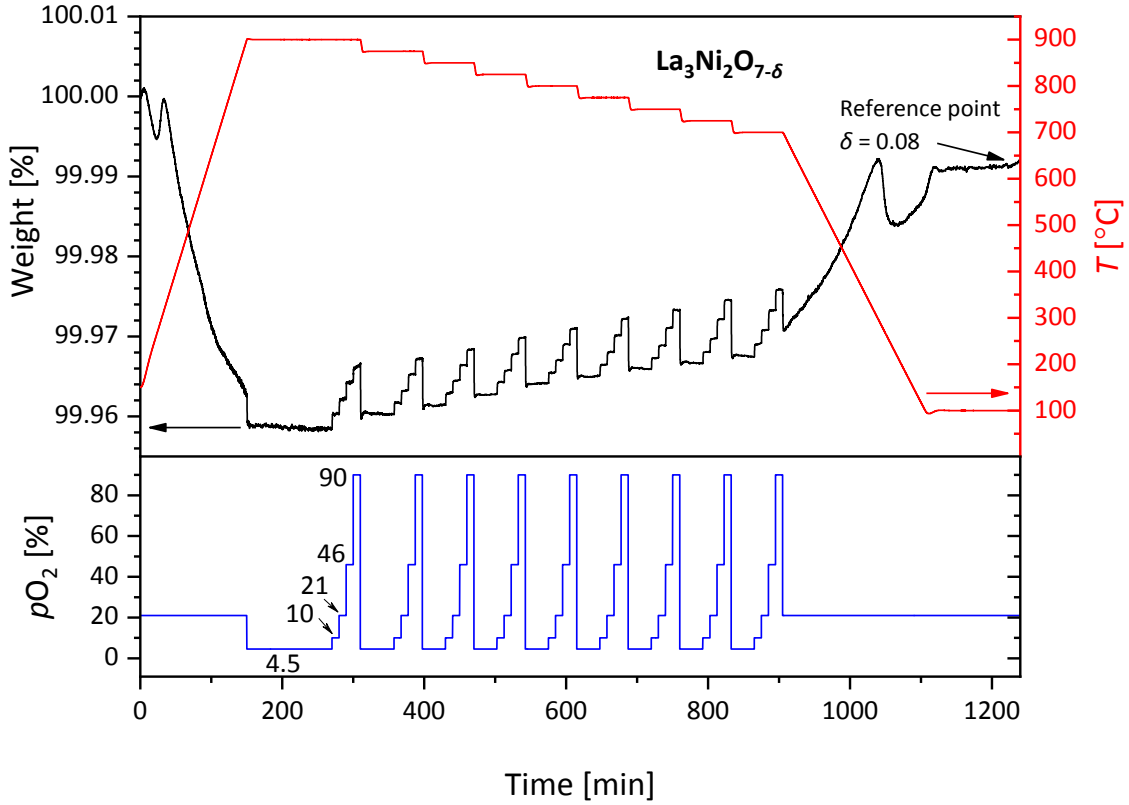

Figure S12 — Weight loss curve for $La_3Ni_2O_{7-\delta}$ on cooling from 900 °C to 700 °C, with intervals of 25 °C, at different pO_2 values. The reference point was selected after equilibration for 3 h at T = 100 °C and pO_2 = 0.21 bar. The corresponding value (δ = 0.08) was determined by reduction in hydrogen (16% H_2/Ar).

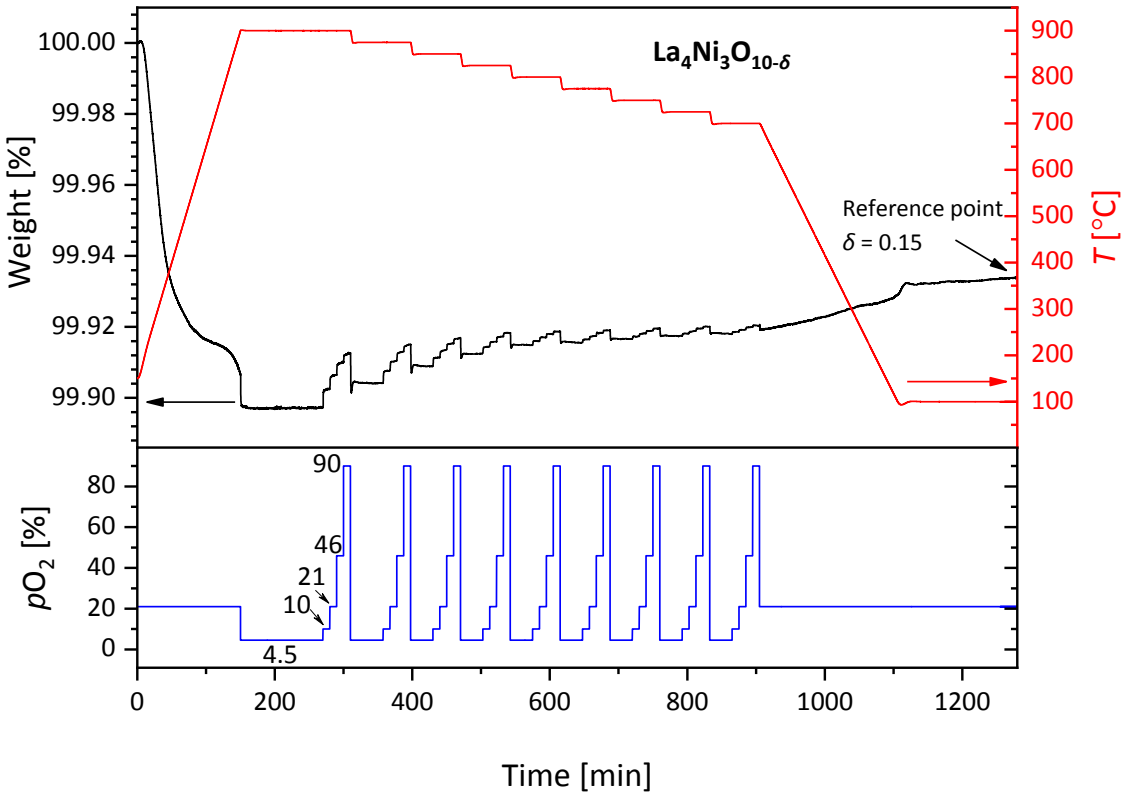

Figure S13 — Weight loss curve for $La_4Ni_3O_{10-\delta}$ on cooling from 900 °C to 700 °C, with intervals of 25 °C, at different pO_2 values. The reference point was selected after equilibration for 3 h at T = 100 °C and pO_2 = 0.21 bar. The corresponding value (δ = 0.15) was determined by reduction in hydrogen (16% H_2/Ar).

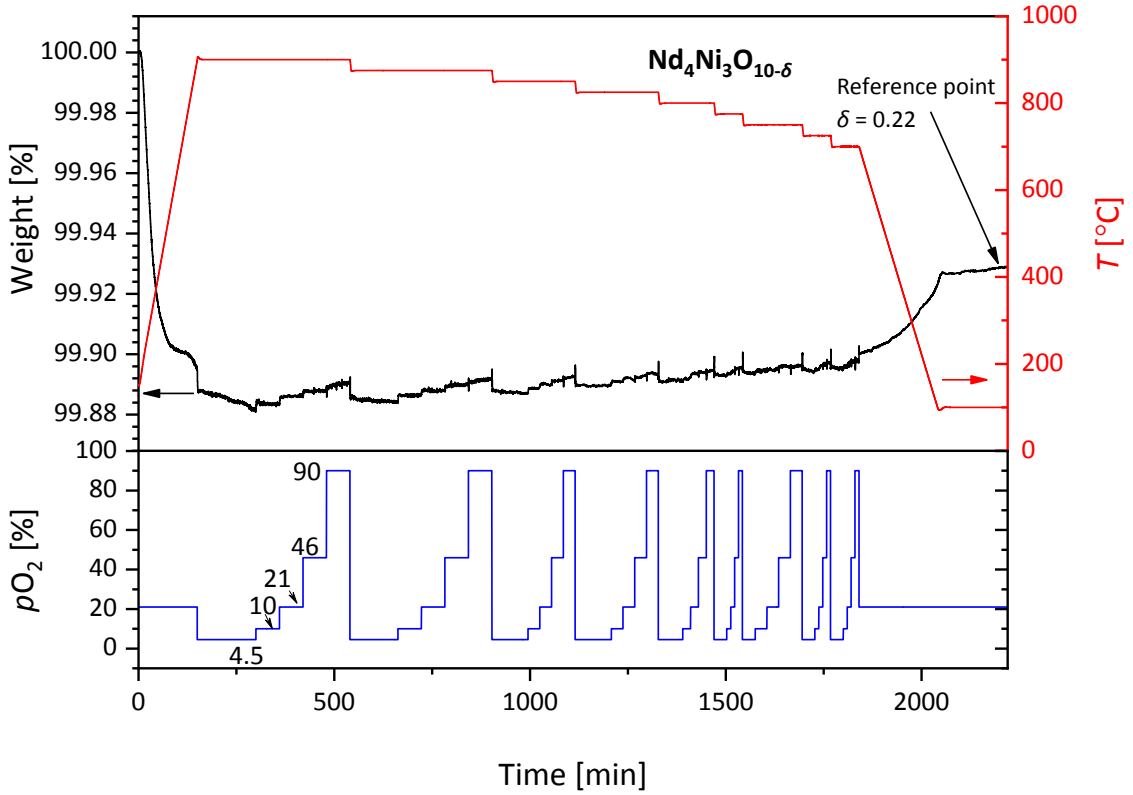

Figure S14 — Weight loss curve for $Nd_4Ni_3O_{10-\delta}$ on cooling from 900 °C to 700 °C, with intervals of 25 °C, at different pO_2 values. The reference point was selected after equilibration for 3 h at T = 100 °C and pO_2 = 0.21 bar. The corresponding value (δ = 0.15) was determined by reduction in hydrogen (16% H_2/Ar).

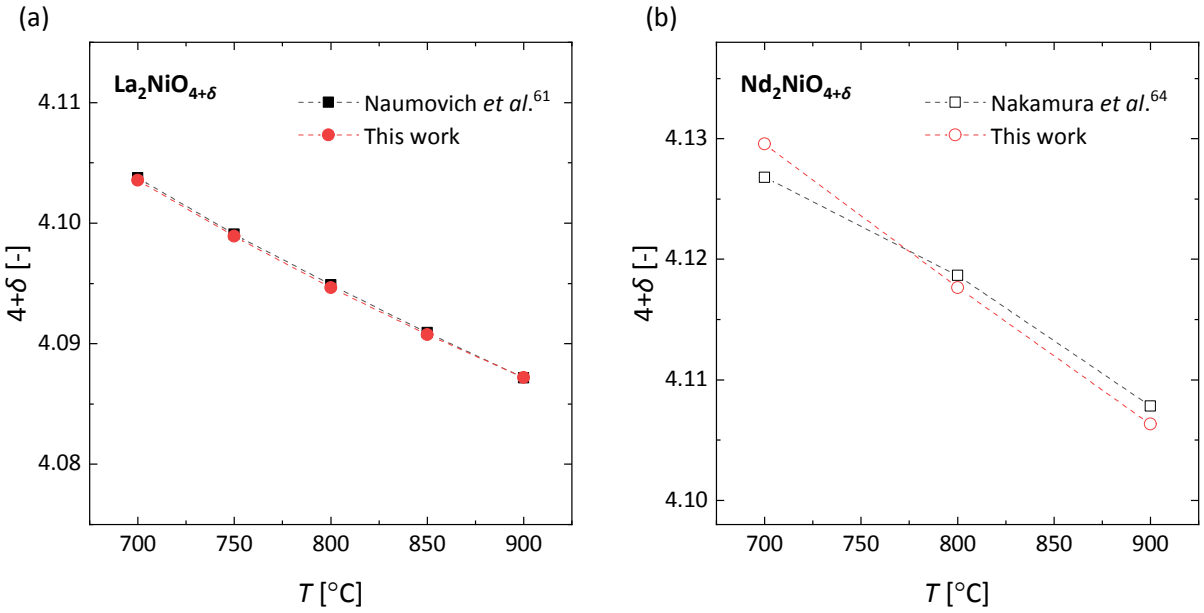

Figure S15 — Comparison of the temperature dependence of the oxygen stoichiometry measured, in air, for (a) $La_2NiO_{4+\delta}$ and (b) $Nd_2NiO_{4+\delta}$ with corresponding data reported in literature.

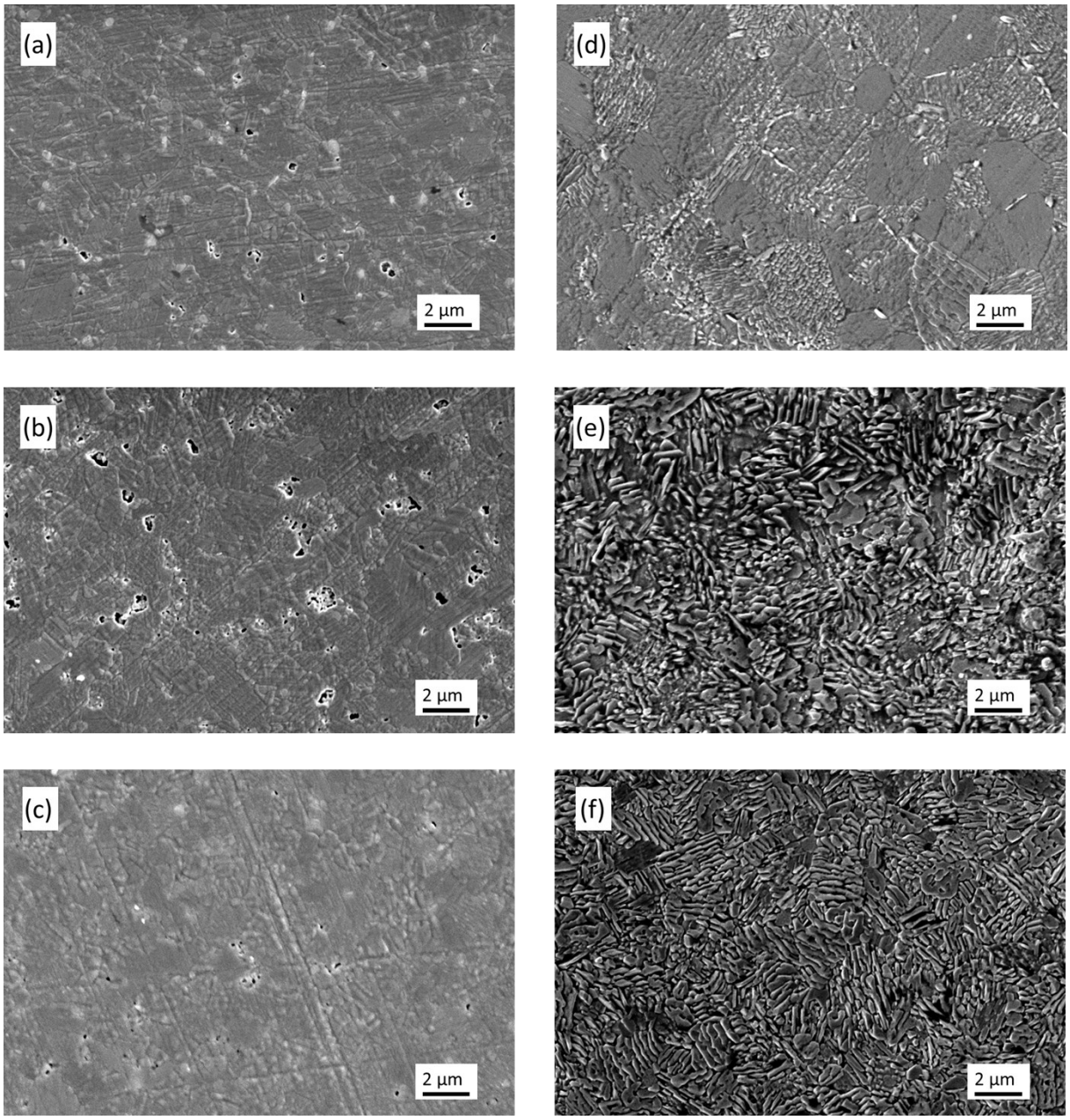

Figure S16 —SEM images of (a, b, c) sintered polished samples, after thermal etching at 1000 °C for 2 h in air, with those of (d, e, f) samples obtained after the ECR experiments for (a, d) $La_2NiO_{4+\delta}$, (b, e) $La_3Ni_2O_{7-\delta}$ and (c, f) $La_4Ni_3O_{10-\delta}$.